Generalized Sampling: A Variational Approach—Part II: Applications

Jan Kybic, *Member, IEEE*, Thierry Blu, *Member, IEEE*, and Michael Unser, *Fellow, IEEE*

***Abstract*—The variational reconstruction theory from a companion paper finds a solution consistent with some linear constraints and minimizing a quadratic plausibility criterion. It is suitable for treating vector and multidimensional signals. Here, we apply the theory to a generalized sampling system consisting of a multichannel filterbank followed by a nonuniform sampling. We provide ready-made formulas, which should permit appliction of the technique directly to problems at hand.**

We comment on the practical aspects of the method, such as numerical stability and speed. We show the reconstruction formula and apply it to several practical examples, including new variational formulation of derivative sampling, landmark warping, and tomographic reconstruction.

***Index Terms*—Reconstruction, sampling, thin-plate splines, variational criterion.**

I. Introduction

In THE first paper of this series [1], we have developed a general theory for reconstructing a signal given a finite set of linear measurements. Since this is in essence an ill-posed problem, we proposed to search for the solution that minimizes some quadratic variational criterion (regularization term) that forces the solution to be smooth. We found the general functional form of the solution to be a linear combination of basis functions derived from the Green's functions of the respective regularization differential operator. By imposing some fundamental invariance properties on the solution (translation, rotation and scale-invariance), we restricted the class of allowable regularization functionals to a one-parameter family that involves iterated Laplacian operator.

In this paper, we will use those theoretical results to explicitly compute the solution of the generalized sampling problem that is schematically represented in Fig. 1. This system is an extended version of the one treated by Papoulis [2]; it allows for nonuniform sampling at arbitrary locations. The general theory [1] does not take explicit advantage of one of its important characteristics: the convolutional form of the measurement process (q-channel filterbank). We will see here that this property translates into a multiwavelet-like form of the solution with one generating function per filter channel (shift-invariant form of the solution).

Manuscript received April 11, 2001; revised May 6, 2002. The associate editor coordinating the review of this paper and approving it for publication was Prof. Fredrik Gustafsson.

J. Kybic was with the Biomedical Imaging Group, DMT/IOA, Swiss Federal Institute of Technology Lausanne, Switzerland. He is now with Robotvis, INRIA, Sophia Antipolis, France (e-mail: kybic@ieee.org).

T. Blu and M. Unser are with the Biomedical Imaging Group, DMT/IOA, Swiss Federal Institute of Technology Lausanne, Switzerland.

Publisher Item Identifier 10.1109/TSP.2002.800386.

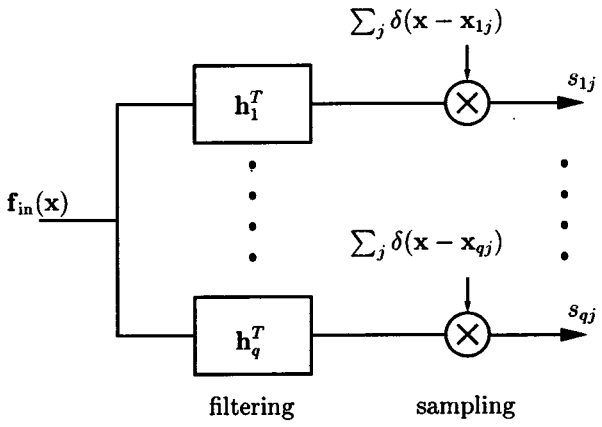

Fig. 1. Generalized sampling. Sampling is modeled as a multiplication with a multidimensional train of Dirac's masses. It yields a set of scalar values s_{ij}. In Papoulis's framework, the sampling is uniform: $x_{ij} = x_j = jT$, and the samples can be grouped to vectors $\mathbf{s}_j$. Here, the sampling locations $\mathbf{x}_{ij}$ can be arbitrary.

Our goal in this paper is twofold. First, we want to bridge the gap between the theoretical formulation in Part I [1] and the effective application of the results to specific sampling cases. We will also simplify the translation from theory to practice by doing a good part of the analytical work—determination of the basis functions and providing computational recipes and implementation formulas that are directly applicable. Second, we consider examples of applications of variational sampling and present some experimental results. We will also emphasize the connection between variational sampling, splines, and radial basis functions.

A. Example of a Variational Interpolation

To motivate the variational approach, let us consider the task of interpolating a unidimensional function. As illustrated in Fig. 2, there is an infinite number of functions passing through the given points. Nevertheless, most people would probably agree that the smooth approximation curve in Fig. 2 looks "more correct" than the rugged noisy approximation. We can often quantify the degree of plausibility of a function for a given application. Then, we search for the most plausible function satisfying our interpolation (consistency) conditions. The plausibility criterion J is the key concept of our approach. From now on, we will concentrate on the typical case where we want the solution to be "smooth." As smoothness can be measured by the amplitude of the derivatives, maximizing smoothness translates into minimizing the norm of various differential operators. In Fig. 2, the smooth curve minimizes the L_2-norm of the second derivative $J(f) = \|f''\|_{L_2}^2$, which is known to

1053-587X/02$17.00 © 2002 IEEE

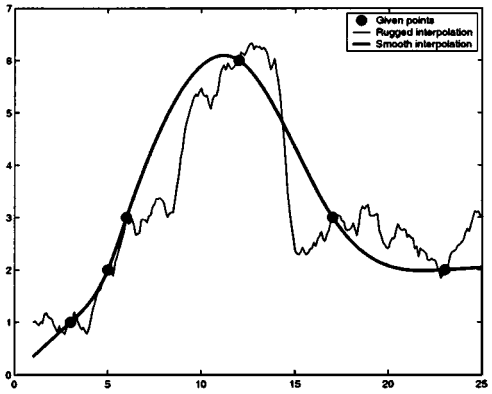

Fig. 2. When interpolating a function from its values (circles), many solutions are possible. However, smooth interpolation (bold line) is usually preferable to a rugged one (thin line).

yield a cubic spline interpolation [3], [4]. A corresponding task of interpolating scalar values in a two-dimensional (2-D) space leads to so-called thin-plate splines [5]–[7].

B. Extensions of the Example

The theory presented in [1] permits several extensions of the simple example above. First, the plausibility (smoothness) criterion can be tailored based on the nature of the underlying data. If, for example, the measures correspond to the position of a body moving with supposedly constant acceleration, then the appropriate criterion should take into account the third derivative f''' instead of f''. Second, instead of the function values (positions), we can conceivably base our reconstruction on other linear measures of the underlying function, such as the derivatives (the speed) or their means across a certain region (average speed). Third, we can also use several of these measures (called *generalized samples*) at the same time, leading to *multichannel* sampling. Finally, the *vector* extension enables us to deal with vector function interpolation, which is frequently encountered in physical systems, permitting treatment of all three spatial coordinates at the same time. All these extensions have been included in the generalized sampling system shown in Fig. 1.

II. Problem Formulation and Solution

This section is designed as a guide to the practitioner for translating the general variational theory [1] into a reconstruction algorithm that is tailored to specific instances of the generalized sampling problem in Fig. 1. At the end of the process, the solution is expressed as a linear combination of continuously defined basis functions with coefficients obtained from the solution of a linear system of equations. Here, we will step through the formulation in some detail and present the key formulas and computations that will be required in practice.

A. Sampling Structure

The generalized sampling in Fig. 1 can be described using a filterbank $\mathtt{H}_{n\times q} = [\mathbf{h}_1 \cdots \mathbf{h}_q]$ consisting of q filters[1] $\mathbf{h}_i$ of size $n \times 1$. At the output of the filterbank, we obtain a set of filtered signals $\mathbf{h}_i^T * \mathbf{f}_{\text{in}}$. We measure (sample) each of the filtered signals at N arbitrary points $\mathbf{x}_{ij}$, which gives a set of qN real samples

$$s_{ij} = \mathbf{h}_i^T * \mathbf{f}_{\text{in}}(\mathbf{x}_{ij}) = \int_{\mathbb{R}^m} \mathbf{h}_i^T(\mathbf{x})\mathbf{f}_{\text{in}}(\mathbf{x}_{ij} - \mathbf{x})\,\mathrm{d}\mathbf{x} \quad (1)$$

for $i \in \{1 \cdots q\}$ and $j \in \{1 \cdots N\}$. This is a special case of the inner-product formulation in [1, Sect. II-C] if we define the following:

$$\mathbf{r}_{i+q(j-1)}(\mathbf{x}) = \mathbf{h}_i(\mathbf{x}_{ij} - \mathbf{x}) \quad \text{and} \quad Nq = Q. \quad (2)$$

We require the reconstruction $\mathbf{f}_{\text{out}}$ to be *consistent*, which means that the signal $\mathbf{f}_{\text{out}}$ must provide exactly the same measurements as the original signal $\mathbf{f}_{\text{in}}$ when run through our measurement system:

$$\left(\mathbf{h}_i^T * \mathbf{f}_{\text{in}}\right)(\mathbf{x}_{ij}) = s_{ij} = \left(\mathbf{h}_i^T * \mathbf{f}_{\text{out}}\right)(\mathbf{x}_{ij}) \quad \forall i \in \{1 \cdots q\}, \quad j \in \{1 \cdots N\}. \quad (3)$$

B. Criterion

Since there is an infinity of signals satisfying (3), we will look for the one that minimizes the plausibility criterion J. To select this criterion, we refer to [1, Th. 1]. We will demand the scale, translation, and rotation invariance of the solution to guarantee that the reconstruction remains the same, regardless of the coordinate system. Together with the requirement of linearity this essentially restricts the choice of the plausibility criterion to Duchon's semi-norms [5], [6] (see [1, Sect.IV-G])

$$J(\mathbf{f}) = \|\mathbf{f}\|_{D_M}^2 = \sum_{i=1}^{N} \|f_i\|_{D_M}^2. \quad (4)$$

The most often used Duchon's semi-norms are summarized in Table I. Table II gives their *kernels* [the functions f for which $J(f) = 0$]: in our case, polynomials of degree $M - 1$. See [1] for general formulas.

The choice of the order of the semi-norm influences the reconstructed function, as shown in Fig. 3. The higher the order, the smoother the solution, but there will be higher overshoot and more pronounced ringing as well.

C. Fundamental Solutions

In our previous paper [1, Th. 2], we show that the solution of the generalized interpolation problem lies in a vector space that is determined by the criterion J and the sampling filterbank $\mathtt{H}$. Its generating (basis) functions $\boldsymbol{\varphi}$: $\mathbb{R}^m \to \mathbb{R}^n$ are called *fundamental solutions*, and they can be obtained by convolution with the sampling operators:

$$[\boldsymbol{\varphi}_1 \cdots \boldsymbol{\varphi}_q] = \boldsymbol{\Phi}_{n\times q} = \boldsymbol{\Psi}_{n\times n} * \mathtt{H}_{n\times q} \quad (5)$$

where the functions ψ are *Green's functions* [8], [9] corresponding to the criterion J. Table III gives the scalar Green's functions for the most often used Duchon's semi-norms as well as in the general case. Note that it is enough to consider the scalar case ($n = 1$); in the vector case ($n > 1$), we get $\boldsymbol{\Psi} = \psi \mathtt{I}_{n\times n}$.

[1]These filters may be distributions. For instance, the identity (no filter) corresponds to Dirac's distribution δ, satisfying $\delta * f = f$.

TABLE I
MOST OFTEN USED DUCHON'S SEMI-NORMS IN DIMENSIONS $m = 1, 2, 3$. M IS THE ORDER OF THE SEMI-NORM. FOR OTHER COMBINATIONS OF m AND M, SEE [1, SECT. IV-G]

$\mathbb{R}^m$	D_M	$\|f\|^2_{D_M}$ for $f : \mathbb{R}^m \to \mathbb{R}$
$\mathbb{R}^1$	D_2	$\int \left(\frac{\mathrm{d}^2 f}{\mathrm{d}x^2}\right)^2 \mathrm{d}x$
$\mathbb{R}^1$	D_3	$\int \left(\frac{\mathrm{d}^3 f}{\mathrm{d}x^3}\right)^2 \mathrm{d}x$
$\mathbb{R}^2$	D_2	$\int \left(\frac{\partial^2 f}{\partial x^2}\right)^2 + 2\left(\frac{\partial^2 f}{\partial x \partial y}\right)^2 + \left(\frac{\partial^2 f}{\partial y^2}\right)^2 \mathrm{d}x\mathrm{d}y$
$\mathbb{R}^2$	D_3	$\int \left(\frac{\partial^3 f}{\partial x^3}\right)^2 + 3\left(\frac{\partial^3 f}{\partial x^2 \partial y}\right)^2 + 3\left(\frac{\partial^3 f}{\partial x \partial y^2}\right)^2 + \left(\frac{\partial^3 f}{\partial y^3}\right)^2 \mathrm{d}x\mathrm{d}y$
$\mathbb{R}^3$	D_2	$\int \left(\frac{\partial^2 f}{\partial x^2}\right)^2 + \left(\frac{\partial^2 f}{\partial y^2}\right)^2 + \left(\frac{\partial^2 f}{\partial z^2}\right)^2 + 2\left(\frac{\partial^2 f}{\partial x \partial y}\right)^2 + 2\left(\frac{\partial^2 f}{\partial x \partial z}\right)^2 + 2\left(\frac{\partial^2 f}{\partial y \partial z}\right)^2 \mathrm{d}x\mathrm{d}y\mathrm{d}z$

TABLE II
KERNELS OF MOST OFTEN USED DUCHON'S SEMI-NORMS IN DIMENSIONS $m = 1, 2, 3$. M IS THE ORDER OF THE SEMI-NORM

$\mathbb{R}^m$	D_M	kernel of $\|f\|^2_{D_M}$ for $f : \mathbb{R}^m \to \mathbb{R}$
$\mathbb{R}^1$	D_2	$a_0 + a_1 x$
$\mathbb{R}^1$	D_3	$a_0 + a_1 x + a_2 x^2$
$\mathbb{R}^2$	D_2	$a_0 + a_1 x + a_2 y$
$\mathbb{R}^2$	D_3	$a_0 + a_1 x + a_2 y + a_3 x^2 + a_4 y^2 + a_5 xy$
$\mathbb{R}^3$	D_2	$a_0 + a_1 x + a_2 y + a_3 z$

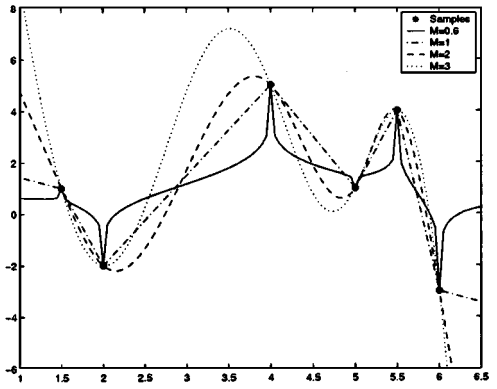

Fig. 3. Dependence of the reconstruction result on the order of the semi-norm M used. High-order semi-norms tend to produce slowly varying curves with large overshoots and vice versa.

D. Explicit Solution

The solution to our generalized interpolation problem, a function $\mathbf{f}_{\text{out}}$ minimizing the criterion (4) under the constraints (3) is given by the following result, which is a restatement of [1, Th. 2] for our particular multichannel system. The main difference is that here, we get one generating function φ_i per channel, which is then shifted to all sampling locations, whereas in [1], we had one function per measurement.

TABLE III
GREEN'S FUNCTIONS ψ IN DIMENSION m CORRESPONDING TO DUCHON'S SEMI-NORM $\|f\|_{D_M}$. THE MULTIPLICATIVE CONSTANTS c, $\hat{c}$ CAN BE DETERMINED BUT ARE IRRELEVANT FOR OUR PURPOSES. THE FUNCTIONS ARE ALL EXPRESSED USING EUCLIDEAN DISTANCE $\rho = \|\mathbf{x}\|$. THE LAST FORMULA IS VALID FOR NONINTEGER α AS WELL

$\mathbb{R}^m$	D_M	$c\,\psi(\mathbf{x})$	$\hat{c}\,\hat{\psi}(\boldsymbol{\omega})$	remark
$\mathbb{R}^1$	D_2	ρ^3	$\|\omega\|^{-4}$	
$\mathbb{R}^1$	D_3	ρ^5	$\|\omega\|^{-6}$	
$\mathbb{R}^2$	D_2	$\rho^2 \log r$	$\|\boldsymbol{\omega}\|^{-4}$	
$\mathbb{R}^2$	D_3	$\rho^4 \log r$	$\|\boldsymbol{\omega}\|^{-6}$	
$\mathbb{R}^3$	D_2	ρ	$\|\boldsymbol{\omega}\|^{-4}$	
$\mathbb{R}^m$	D_α	$\rho^{2\alpha-m} \log \rho$	$\|\boldsymbol{\omega}\|^{-2\alpha}$	if $2\alpha - m$ is even
$\mathbb{R}^m$	D_α	$\rho^{2\alpha-m}$	$\|\boldsymbol{\omega}\|^{-2\alpha}$	otherwise

Theorem 1 (Interpolation Problem Solution): The generalized interpolation problem is solved by a function

$$\mathbf{f}_{\text{out}}(\mathbf{x}) = \underbrace{\sum_{k=0}^{P-1} a_k \mathbf{p}_k}_{\text{kernel part}} + \underbrace{\sum_{i=1}^{q} \sum_{j=1}^{N} \lambda_{ij} \varphi_i(\mathbf{x} - \mathbf{x}_{ij})}_{\text{fundamental part}} \tag{6}$$

where φ_i are the fundamental solutions, and $\{\mathbf{p}_k\}_{k=0}^{P-1}$ is the basis of the kernel of the semi-norm J (e.g., polynomials), if and only if the following three conditions are satisfied.

i) The solution $\mathbf{f}_{\text{out}}$ is consistent with the constraints

$$s_{ij} = \mathbf{h}_i^T * \mathbf{f}_{\text{out}}(\mathbf{x}_{ij}) \qquad \text{for all } i, j. \tag{7}$$

ii) The coefficients λ_{ij} satisfy the "orthogonality" condition

$$\sum_{ij} \lambda_{ij} \left(\mathbf{h}_i^T * \mathbf{p}_k\right)(\mathbf{x}_{ij}) = 0 \qquad \text{for all } k. \tag{8}$$

iii) The solution $\mathbf{f}_{\text{out}}$ is admissible, i.e., $J(\mathbf{f}_{\text{out}}) < \infty$. □

The condition iii) is usually ensured by the coefficients obtained in i) and ii).

Equivalently, i) and ii) can be written in a matrix form as

$$\underbrace{\begin{bmatrix} \mathtt{A} & \mathtt{Q} \\ \mathtt{Q}^T & \mathbf{0} \end{bmatrix}}_{\mathtt{B}} \begin{bmatrix} \boldsymbol{\lambda} \\ \mathbf{a} \end{bmatrix} = \begin{bmatrix} \mathbf{s} \\ \mathbf{0} \end{bmatrix} \tag{9}$$

where the parameters have been arranged in vectors as $\boldsymbol{\lambda} = [\lambda_{1,1} \cdots \lambda_{1,N}\ \lambda_{2,1} \cdots \lambda_{q,N}]^T$ and $\mathbf{a} = [a_1 \cdots a_P]^T$. The components of the matrix $\mathtt{A}$ of size $Nq \times Nq$ are given by $(\mathtt{A})_{iN+k,\,jN+l} = \mathbf{h}_i^T * \boldsymbol{\varphi}_j(\mathbf{x}_{ik} - \mathbf{x}_{jl})$ and represent the contribution of the fundamental solutions to each measurement. The components of the matrix $\mathtt{Q}$ are given by $(\mathtt{Q})_{iN+j,\,k} = \mathbf{h}_i^T * \mathbf{p}_k(\mathbf{x}_{ij})$ and represent the kernel part of the solution as well as the orthogonality conditions.

We see that (6) consists of two parts. The first (the kernel part) does not contribute to the criterion $J(\mathbf{f}+\mathbf{p}_k) = J(\mathbf{f})$; therefore, we can intuitively tell that it is useful to accommodate in it as much as possible of $\mathbf{f}_{\text{out}}$. In fact, the orthogonality conditions ii) ensure that the fundamental part of the solution (6) is orthogonal to any element of the kernel.

The second, fundamental part of the solution consists of a linear combination of shifted basis functions $\boldsymbol{\varphi}_j$ positioned at the sampling points. Interestingly, the fundamental part is reminiscent of a wavelet (or multiwavelet) like expansion because it also involves shifts of some generating functions. One difference is that here, the basis functions $\boldsymbol{\varphi}_i(\mathbf{x} - \mathbf{x}_{ij})$ in (6) are not necessarily uniformly spaced. Another difference is that wavelets are usually well localized, whereas the functions $\boldsymbol{\varphi}_i$ [related by convolution (5) to the Green's functions ψ from Table III] are typically not since they increase as one moves away from the origin. However, the orthogonality conditions (8) localize the functions $\mathtt{L}^T * \boldsymbol{\varphi}_i$ (where $J(\mathbf{f}) = \|\mathtt{L}^T * \mathbf{f}\|^2$; see [1, Sect. III-E]), which has the effect of taming the growth of the solution at infinity. Dropping the scale-invariance requirement leads to basis functions that grow more slowly [10].

E. Numerical Aspects

The presented method requires the solution of a large, nonsparse system of equations. Additional research is required to develop fast numerical solvers [11], such as specialized iterative methods [12], [13]. A related aspect is the ill conditioning of the system matrix due to the nonlocal nature of the basis functions. We believe this can be improved using adequate preconditioners, e.g., by localizing the basis functions, similar to the construction of B-spline basis [14]. Other techniques include domain decomposition [15] or algebraic manipulation suitable for special form of the matrices [16, Ch. 4].

F. Generalized Approximation Problem

In some applications, for example, if the measurements are noisy, we do not want the reconstructed function $\mathbf{f}_{\text{out}}$ to pass exactly through the measured points. Instead, we want it to be a compromise between its smoothness (or plausibility), as measured by the criterion J, and the closeness of the fit to the sampled points, as measured for example by the sum of the squared differences. In a *generalized approximation problem* [1, Sect. VI], we minimize a combined criterion J_a. For the standard regularized least-squares approximation, J_a has the form

$$J_a(\mathbf{f}) = J(\mathbf{f}) + \gamma \underbrace{\sum_{ij} \left(\mathbf{h}_i^T * \mathbf{f}(\mathbf{x}_{ij}) - s_{ij}\right)^2}_{\text{data term } J_d} \tag{10}$$

where J is the regularization criterion defined by (4), and s_{ij} are the measured points close to which we want to pass. The problem is equivalent to finding a $\mathbf{f}_{\text{out}}$ that minimizes J under the constraint $J_d \leq \varepsilon$, where ε is an *a priori* given error bound. The γ should be chosen such that the error ε correspond to the expected noise (error) in the measurements. If the measurement noise is not known, a suitable γ can be found, for example, using the leave-one-out technique [17].

The solution of the approximation problem (see [1, Th. 3 and its sequels]) has the same form $\mathbf{f}_{\text{out}}$ defined by (6), and the parameters a_i and λ_{ij} satisfy the matrix equation

$$\underbrace{\begin{bmatrix} \mathtt{A} + \gamma^{-1}\mathtt{I} & \mathtt{Q} \\ \mathtt{Q}^T & \mathbf{0} \end{bmatrix}}_{\mathtt{B}} \begin{bmatrix} \boldsymbol{\lambda} \\ \mathbf{a} \end{bmatrix} = \begin{bmatrix} \mathbf{s} \\ \mathbf{0} \end{bmatrix} \tag{11}$$

where the symbols are the same as in (9).

The simplicity of (11) is a consequence of the continuous regularization and of using the fundamental solutions as the basis of our space. Our variational formulation of the approximation problem is similar in spirit to using discrete regularization [18]–[20] to deal with the ill-poseness of some inverse problems. Our regularization, however, is completely specified in the continuous domain. In addition, those discrete regularizations, which are often used in combination with nontrivial basis functions, such as the finite element method (FEM), modify the equation set in a much more complicated and less predictable way. The identity matrix $\mathtt{I}$ is replaced by some general matrix that needs to be determined on a case-by-case basis.

III. Examples

We now give various examples of how the theory can be used and present some experimental results.

A. Reconstruction from Irregular Samples

Let us consider the problem of finding a function $f: \mathbb{R} \to \mathbb{R}$ passing through a finite number of points (x_i, y_i) and minimizing a criterion $J(f) = \|f\|_{D_2}^2 = \|f''\|^2$ (see Table I). From Table III, we see that the fundamental solution corresponding to the semi-norm J is proportional to $|x|^3$. The kernel corresponding to this semi-norm is the class of all linear polynomials $a_0 + a_1 x$, i.e., the class of functions for which $f'' = 0$ everywhere. The reconstruction is thus

$$f(x) = a_0 + a_1 x + \sum_{i=1}^{N} \lambda_i |x - x_i|^3 \tag{12}$$

which has $N + 2$ unknown parameters. The consistency conditions $f(x_i) = y_i$ give us N linear equations, whereas the orthogonality requirements $\sum \lambda_i = 0$ and $\sum \lambda_i x_i = 0$ yield the remaining two. A nice consequence of the orthogonality conditions is to make the second derivative $f''(x) = 6 \sum_i \lambda_i |x - x_i|$

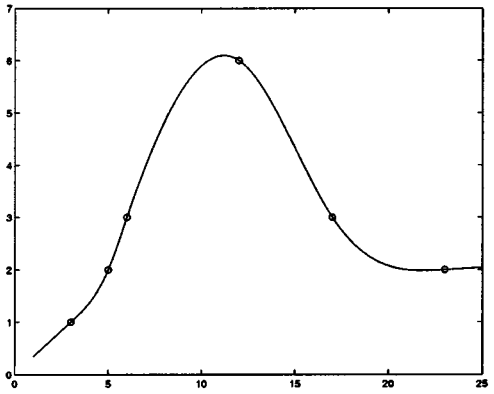

Fig. 4. Interpolation from function values.

vanish after the last sampling point, which ensures that $J(f) < \infty$, and thus, $f \in F$. Note that f is a piecewise cubic polynomial with continuous second derivatives, i.e., it is a *cubic spline*. This result is known, see [3] and [21]. An example of a spline reconstruction (interpolation) is shown in Fig. 4.

For uniform sampling, the basis functions $|x - x_i|^3$ can be localized using digital filtering (with iterated finite difference filter) to obtain compactly supported uniform cubic B-splines, which makes an interesting link with existing theory [22], [23]. For nonuniform sampling, the localization is also possible using divided differences [24], leading to nonuniform B-splines. In both cases, if we increase the order M of the semi-norm, the order of the splines will increase as well, and the corresponding interpolation will converge to the sinc interpolation [25], [26]. This shows the relation with the classical sampling theorem [27].

B. Smoothing Splines

If the measured points from the preceding example are not exact, it is more appropriate to replace interpolation by approximation (see Section II-F). The reconstruction formula (12) remains, whereas the equation set (9) used to determine the parameters a_i and λ_i is now replaced by the equation set (11). An example of a result for the same sampled points as before is shown in Fig. 5. The smoothing spline method that we have just described is a nonparametric regression technique widely used in statistics [28].

C. Derivative Sampling

Let us add derivative constraints $y'_i = f'(x_i)$ to the example from Section III-A. The sampling filters will become $\mathrm{H} = [\delta \; \delta']$. The first fundamental solution corresponding to $h_1 = \delta$ remains $\varphi_1 = c|x|^3$. The second one, corresponding to $h_2 = \delta'$, is obtained by convolving φ_1 with h_2, which gives $\varphi_2 = 3c|x|x$. The reconstruction formula is thus

$$f_{\text{out}}(x) = a_0 + a_1 x + \sum_{i=1}^{N} \lambda_{i,1}|x - x_i|^3 + 3\lambda_{i,2}|x - x_i|(x - x_i).$$

The $2N + 2$ unknown parameters can be determined from $2N$ consistency equations $f(x_i) = y_i$ and $y'_i = f'(x_i)$ and two

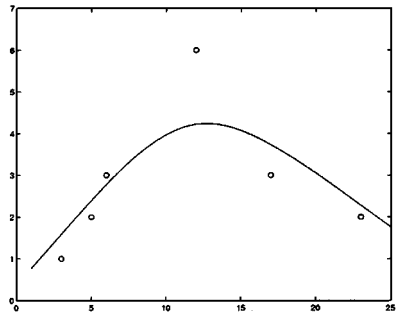

Fig. 5. Approximation between given points for $\gamma = 10^{-3}$.

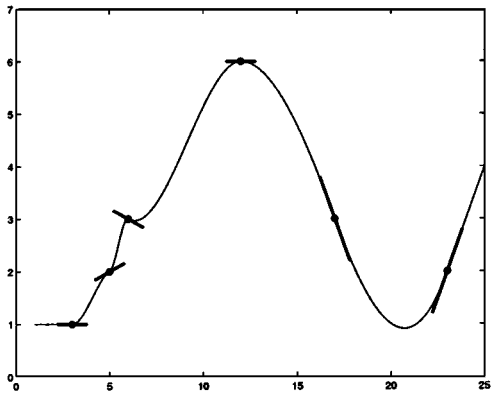

Fig. 6. Interpolation from function values and derivatives.

orthogonality conditions $\sum \lambda_{i,1} = 0$ and $\sum \lambda_{i,2} + \lambda_{i,1} x_i = 0$. These orthogonality conditions come from the requirement (8) that $\sum_i \lambda_{i,1} p_k(x_i) + \lambda_{i,2} p'_k(x_i) = 0$, where $p_1 = 1, p_2 = x$ is the basis of the kernel. An example of reconstruction from derivative sampling is shown in Fig. 6. A trivial extension is to sample the derivative values at different points than the function values.

D. Landmark-Based Warping

The problem of image registration is encountered in many areas of image processing. The task is to find correspondences between pixel coordinates in two distinct but similar images. In other words, we search for a function that gives us, for each point in the first image, the coordinates of the corresponding point in the second image. In some cases, it is necessary to use manual methods [29]. These mostly require the expert to specify a set of pairwise corresponding landmarks [7] (reference points) in both images. Then, an interpolation method is needed to also find the deformation function between the landmarks, which is exactly the problem studied in this paper. Supposing we want to find the 2-D deformation function minimizing Duchon's semi-norm of order two, we see from Table III that we need to interpolate using the $\rho^2 \log \rho$ functions, which are also called thin-plate splines.

Fig. 7 shows an example where landmark warping is used to compensate distortion in functional magnetic resonance imaging (fMRI) images by registration with anatomically correct (proton density) MR images [30]. More examples of landmark interpolation using different interpolating functions

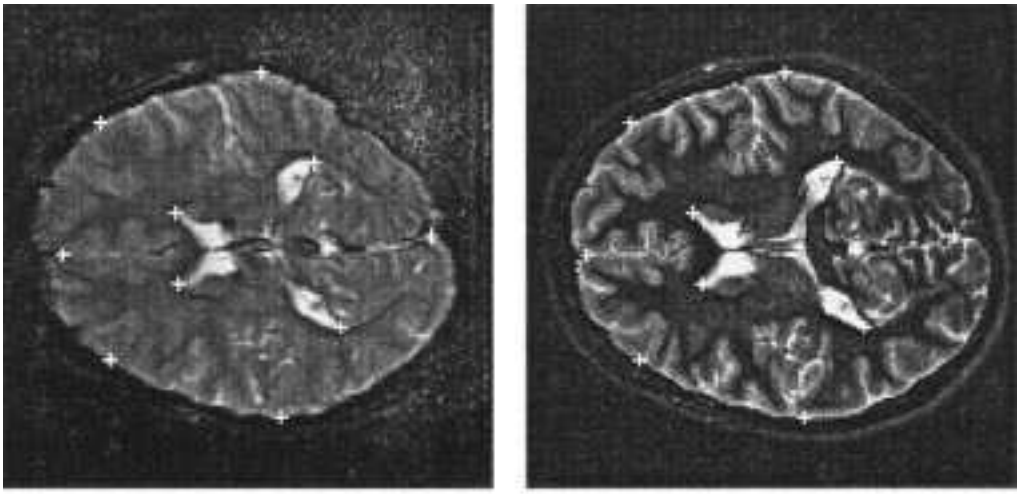

Fig. 7. Corresponding slices of (a) functional MR and (b) anatomical (proton density) MR images with landmarks put manually at important points. The deformation field between landmarks is determined by interpolation using variational reconstruction method (equivalent to thin-plate splines in this case).

can be found in [31]. Some demonstrations are available on our web page http://bigwww.epfl.ch/demo.

E. Reconstruction Consistent With Laplace Equation

The problem treated in [32] by numerical integration—which we will solve explicitly here—consists of reconstructing a function $\mathbb{R}^3 \rightarrow \mathbb{R}$, minimizing the norm of the 3D Laplacian operator $J_\Delta(f)^2 = \int_{\mathbb{R}^3} ||\Delta f||^2 \, \mathrm{d}\mathbf{x}$. The problem is ill-posed without additional constraints because the kernel $\mathcal{K}_\Delta$ is too big, including all functions that satisfy Laplace's equation $\Delta f = 0$, such as $x^2 - y^2$. It therefore permits an infinity of solutions with zero cost. To avoid this ambiguity, we will instead minimize a criterion $J(f) = ||f||_{D_2}$, the explicit expression of which can be found in Table I. This makes sense because when f is well behaved, the two criteria J and J_Δ are equal. The corresponding fundamental solution is $\varphi(\mathbf{x}) = \rho$ (where $\rho = ||\mathbf{x}||$). Since the kernel consists of linear polynomials, the solution takes the form

$$f_{\text{out}}(\mathbf{x}) = \begin{bmatrix} a_0 & a_1 & a_2 & a_3 \end{bmatrix} \begin{bmatrix} 1 \\ \mathbf{x} \end{bmatrix} + \sum_{i=1}^{N} \lambda_i ||\mathbf{x} - \mathbf{x}_i|| \quad (13)$$

with the auxiliary conditions $\sum_i \lambda_i = 0$, and $\sum_i \lambda_i x_i = \sum_i \lambda_i y_i = \sum_i \lambda_i z_i = 0$ for $j = 1, 2, 3$, where $\mathbf{x}_i = [x_i \;\; y_i \;\; z_i]^T$ are the coordinates of the ith measurement point. As before, the coefficients a_i and λ_i must be determined in such a way that f_{out} passes by the desired points.

F. Derivative Sampling in Two Dimensions

Adding another level of complexity, we are going to extend the derivative sampling from Section III-C to two dimensions. The task is to find a function f: $\mathbb{R}^2 \rightarrow \mathbb{R}$ given its values $f(\mathbf{x}_i)$ as well as the values of its first partial derivatives $\nabla_{\mathbf{x}} f(\mathbf{x}_i)$ at sampling points $\mathbf{x}_i = [x_i \; y_i]^T$. Our analysis filters are therefore

$$\mathrm{H} = \begin{bmatrix} \delta & \dfrac{\partial \delta}{\partial x} & \dfrac{\partial \delta}{\partial y} \end{bmatrix}.$$

For reasons given later, we choose f that minimizes $J(f) = ||f||_{D_3}$. The kernel of this criterion consists of bivariate polynomials of degree less than or equal to 2, and its Green's function (see Table III) is $\psi(\mathbf{x}) = c \, \rho^4 \log \rho$. Consequently, the fundamental solutions φ_i corresponding to the three sampling filters are, respectively, ψ, and its partial derivatives with respect to both x and y.

This means that the solution f_{out}, besides the term from the kernel, consists of a linear combination of shifted fundamental solutions [see (6)]

$$f_{\text{out}}(x, y) = a_0 + a_1 x + a_2 y + a_3 x^2 + a_4 y^2 + a_5 xy + \sum_{i=1}^{N} \boldsymbol{\lambda}_i^T \begin{bmatrix} \psi(\mathbf{x} - \mathbf{x}_i) \\ \dfrac{\partial \psi}{\partial x}(\mathbf{x} - \mathbf{x}_i) \\ \dfrac{\partial \psi}{\partial y}(\mathbf{x} - \mathbf{x}_i) \end{bmatrix} \quad (14)$$

where $\boldsymbol{\lambda}_i = [\lambda_{i,1} \; \lambda_{i,2} \; \lambda_{i,3}]^T$. There are six orthogonality constraints [from (8)] corresponding to the six basis functions of the kernel

$$1\text{:} \sum_i \lambda_{i,1} = 0$$

$$x\text{:} \sum_i x_i \lambda_{i,1} + \lambda_{i,2} = 0 \qquad y\text{:} \sum_i y_i \lambda_{i,1} + \lambda_{i,3} = 0$$

$$x^2\text{:} \sum_i x_i^2 \lambda_{i,1} + 2 x_i \lambda_{i,2} = 0 \quad y^2\text{:} \sum_i y_i^2 \lambda_{i,1} + 2 y_i \lambda_{i,3} = 0$$

$$xy\text{:} \sum_i x_i y_i \lambda_{i,1} + y_i \lambda_{i,2} + x_i \lambda_{i,3} = 0.$$

Note that some care is needed in selecting the regularization criterion J. Had we chosen the classical criterion $||f||_{D_2}$, we would have obtained $\psi(\mathbf{x}) = \rho^2 \log \rho$ as the fundamental solution, the second derivative of which is not bounded around zero, thus preventing the evaluation of the measures $\nabla_{\mathbf{x}} f_{\text{out}}(\mathbf{x}_i)$ of (14) at

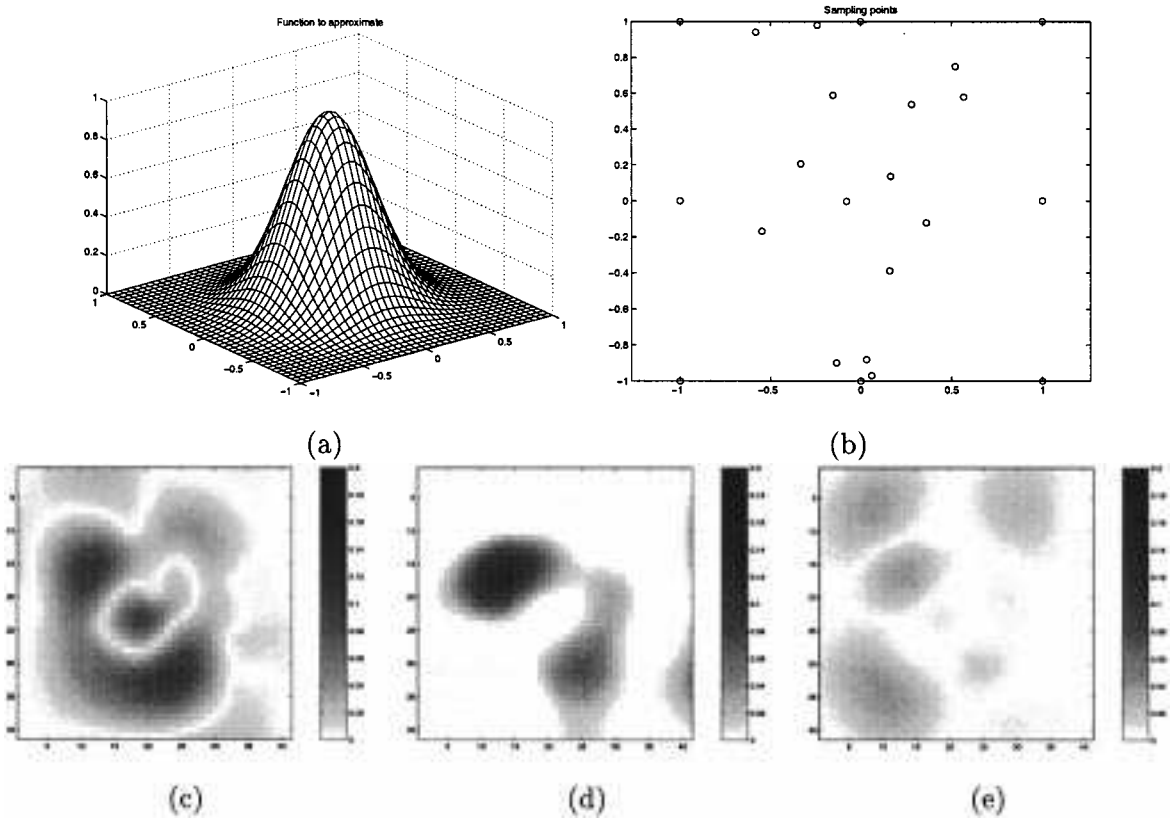

Fig. 8. Reconstructing a 2-D Gaussian (a) from information at sampling points (b). The difference between the true function and the approximation gets progressively smaller as we use (c) thin-plate spline $r^2 \log r$ approximation, (d) approximation using $r^4 \log r$, and (e) approximation using $r^4 \log r$ with measurements of derivatives. The respective SNRs are (c) 13.4 dB, (d) 18.7 dB, and (e) 34.2 dB. The approximation using derivatives gives the best results. Bear in mind, however, that the derivative method uses an extra information (the derivatives) that the other methods cannot use.

grid points. No such (nontrivial) f_{out} would belong to F; the problem would not admit a solution in F.

As an example, we have approximated a 2-D Gaussian using thin-plate splines and $r^4 \log r$ functions both with and without the derivative information. The results are shown in Fig. 8. The higher order approximation with $r^4 \log r$ functions leads to a smoother function than the thin-plate spline solution ($r^2 \log r$) and, therefore, performs better for approximating a Gaussian that is a very smooth function. Not surprisingly, the method using the derivatives we have just described gives the best results.

This approach can be easily extended for finding vector functions $\mathbf{f}$: $\mathbb{R}^2 \rightarrow \mathbb{R}^2$ by taking $J(\mathbf{f}) = J(f_x) + J(f_y)$, where $(f_x, f_y) = \mathbf{f}$ are the components of $\mathbf{f}$. As the components are treated separately, the solution can be calculated independently for each of them. One possible application is semi-automatic landmark image warping with derivative constraints.

G. Tomographic Reconstruction

A nice example of a classic inverse problem that also falls into our framework is tomographic reconstruction [33], [34]. It consists of reconstructing a cross section of an object from its transaxial projections. We now show that tomographic reconstruction lends itself well to the variational formulation. Alternative algorithms involve wavelets [35] and polynomial convolutional kernels [36].

Let $f(x, y)$ be the unknown cross section of the object to be reconstructed. We measure the projections of f at q angles θ_i. For each angle, we measure an integral along a ray at N positions u_j, that is

$$s_{ij} = \int_{\mathbb{R}} f(t \cos\theta_i - u_j \sin\theta_i,\ t \sin\theta_i + u_j \cos\theta_i)\, \mathrm{d}t. \quad (15)$$

This integral corresponds to our sampling operator. The variational formulation of the reconstruction problem is thus: Find a function f_{out} consistent with measurements s_{ij} [yielded by (15)] and minimizing a plausibility criterion J. We choose J to be Duchon's semi-norm $J(f) = \|f\|_{D_2}$.

The projection/sampling operator (15) can be written as a convolution

$$\begin{aligned} s_{ij} &= \langle \delta(x \sin\theta_i - y \cos\theta_i + u_j),\ f \rangle \\ &= \left(\underbrace{\delta(-x \sin\theta_i + y \cos\theta_i)}_{h_i} * f \right) \left(\underbrace{-\sin\theta_i u_j,\ \cos\theta_i u_j}_{\mathbf{x}_{ij}} \right). \end{aligned} \quad (16)$$

The fundamental solution φ_i for the sampling operator (16) needs to satisfy the defining equations from [1, Sect. V-D], which in this case lead to

$$\Delta^2 \varphi_i(x, y) = \delta(-x \sin\theta_i + y \cos\theta_i). \quad (17)$$

To find φ_i, we rotate our coordinate system by $-\theta_i$, which yields a 1-D problem equivalent to the one in Section III-A with solutions $|x'|^3$. In our 2-D case, after rotating the coordinate system back, we get

$$\varphi_i = |-\sin\theta_i x + \cos\theta_i y|^3. \quad (18)$$

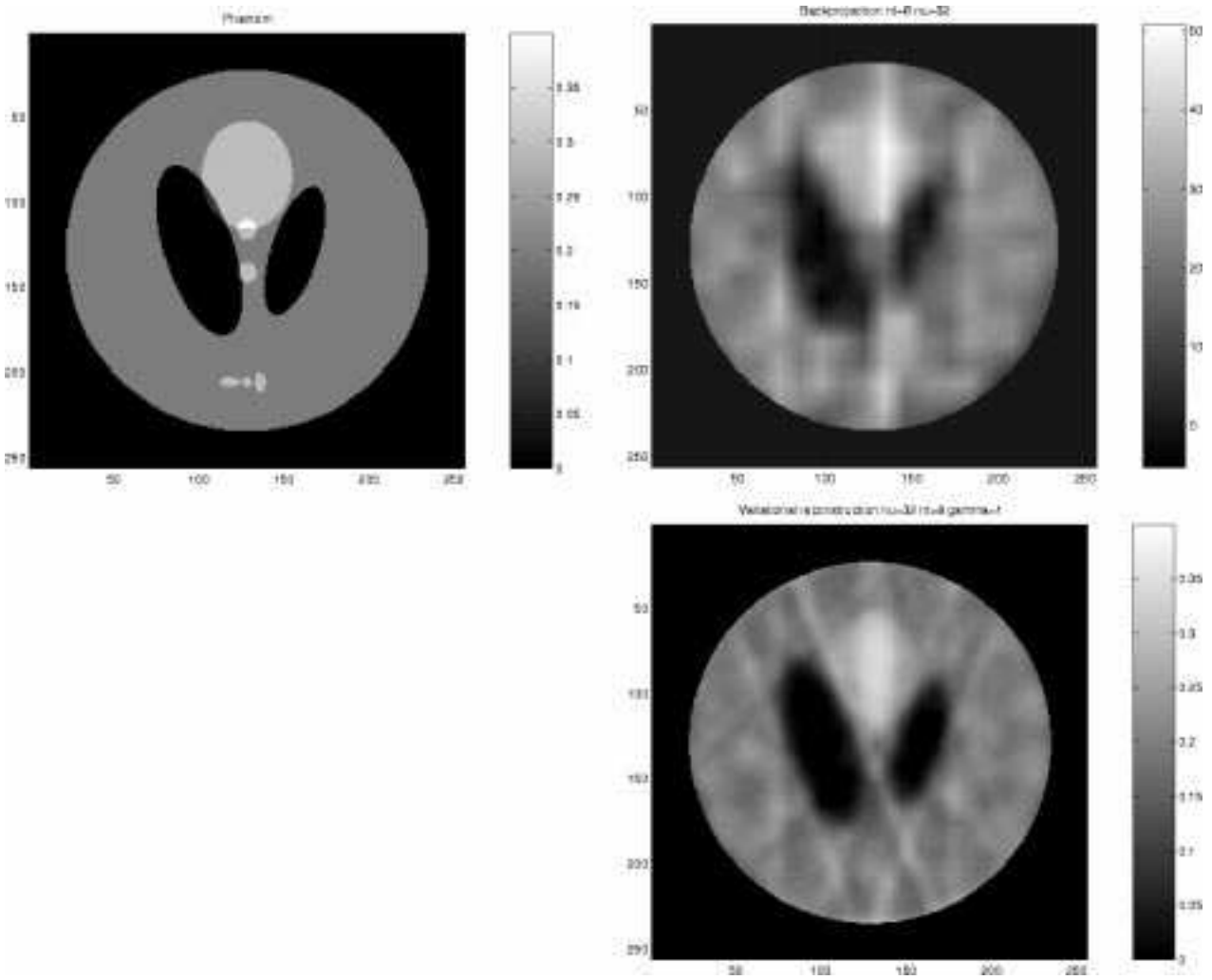

Fig. 9. We are reconstructing the inner part of the Shepp and Logan phantom [33] (top left), using projections at eight uniformly distributed angles, 32 measurements by angle. The result of the filtered backprojection (top right) has more artifacts and is less geometrically precise than the variational reconstruction (bottom right). In addition, note that unlike filtered backprojection, the variational reconstruction recovers the absolute amplitudes in the image well.

Putting the pieces together, we find that our reconstruction takes the form

$$f_{\text{out}}(x, y) = \begin{bmatrix} a_0 & a_1 & a_2 \end{bmatrix} \begin{bmatrix} 1 \\ x \\ y \end{bmatrix} + \sum_{j=1}^{q} \sum_{i=1}^{N} \lambda_{ij} |-x \sin\theta_i + y \cos\theta_i - u_j|^3. \quad (19)$$

The interesting thing is the structure of the generating functions φ_i that are back-projections (extensions) of the corresponding 1-D fundamental solutions along the projection rays. They have the same form as in the standard backprojection algorithm [33].

For a more realistic application, we consider that the measurements $\mathbf{s}$ are noisy, and we therefore use the approximation formulation from Section II-F. Second, instead of integrating over the whole space in (15) and (16), we only integrate over the part corresponding to the measurement device. If we also evaluate the regularization criterion in the same domain, the fundamental solutions φ_i remain the same.

Fig. 9 shows a comparison of the reconstruction using the variational algorithm and classical filtered backprojection [33], as implemented in Matlab. We can observe that for a small number of measurements, the variational reconstruction algorithm gives a better result than the filtered backprojection. For a large number of measurements, the results of the variational reconstruction are comparable with that of the filtered backprojection. Thus, our method is especially useful in the case of few angles. More details can be found in [37].

IV. Conclusions

We have presented an interpolation and approximation scheme capable of treating nonuniformly sampled multichannel output of a filterbank. The reconstruction is optimal in the sense of a user-chosen criterion. The method is easily modifiable to adapt to various sampling (measuring) systems and can take advantage of an *a priori* knowledge about the reconstructed object.

We present mathematical recipes that should facilitate the derivation of the relevant formulas for specific problems and the subsequent use of the variational reconstruction.

We believe that our reconstruction algorithm is especially useful for applications where there are few measurements as it permits to use them in the best possible way. We have presented several examples to illustrate its possible uses.

REFERENCES

[1] J. Kybic, T. Blu, and M. Unser, "Generalized sampling: A variational approach. Part I—Theory," *IEEE Trans. Signal Processing*, vol. 50, pp. 1965–1976, Aug. 2001.

[2] A. Papoulis, "Generalized sampling expansion," *IEEE Trans. Circuits Syst.*, vol. CAS–24, pp. 652–654, 1977.

[3] J. H. Ahlberg, E. N. Nilson, and J. L. Walsh, *The Theory of Splines and Their Applications*. New York: Academic, 1967.

[4] I. J. Schoenberg, "Spline functions and the problem of graduation," *Proc. Nat. Acad. Sci.*, vol. 52, pp. 947–950, 1964.

[5] J. Duchon, "Splines minimizing rotation-invariant semi-norms in Sobolev spaces," in *Constructive Theory of Functions of Several Variables*, W. Schempp and K. Zeller, Eds. Berlin, Germany: Springer-Verlag, 1977, pp. 85–100.

[6] J. Duchon, "Interpolation des fonctions de deux variables suivant le principe de la flexion des plaques minces," *Rev. Française d'Automat., Inform. Recherche Oper.*, vol. 10, no. 12, pp. 5–12, Dec. 1976.

[7] F. Bookstein, *Morphometric Tools for Landmark Data: Geometry and Biology*. Cambridge, U.K.: Cambridge Univ. Press, 1997.

[8] D. G. Duffy, *Green's Functions With Applications*. Boca Raton, FL: Chapman & Hall/CRC, 2001, Studies in Advances Mathematics.

[9] G. Barton, *Elements of Green's Functions and Propagation*. New York: Oxford Univ. Press, 1989.

[10] M. Gabrani and O. J. Tretiak, "Surface-based matching using elastic transformations," *Pattern Recognit.*, no. 32, pp. 87–97, 1999.

[11] M. D. Buhmann, "Radial basis functions," *Acta-Numerica*, vol. 9, pp. 1–38, 2000.

[12] R. K. Beatson and G. Newsam, "Fast evaluation of radial basis functions: I," *Comput. Math. Applicat.*, vol. 24, no. 12, pp. 7–19, 1992.

[13] R. K. Beatson and M. J. D. Powell, "An iterative method for thin-plate spline interpolation that employs approximations to the Lagrange functions," in *Numerical Analysis 1993*, D. F. Griffiths and G. A. Watson, Eds. Essex, U.K.: Longman Scientific, 1994, pp. 17–39.

[14] C. de Boor, *A Practical Guide to Splines*. New York: Springer-Verlag, 1978.

[15] R. K. Beatson, W. A. Light, and S. Billings, "Fast solution of the radial basis function interpolation equations: Domain decomposition methods," *SIAM J. Sci. Comput.*, vol. 2, no. 5, pp. 1717–1740, 2000.

[16] A. Stenman, "Model on demand: Algorithms, analysis and applications," Ph.D. dissertation, Dept. Elect. Eng., Linköping Univ., Linköping, Sweden, Apr. 1999.

[17] D. M. Allen, "The relationship between variable selection and data augmentation and a method for prediction," *Technomet.*, vol. 1, no. 16, pp. 125–127, 1974.

[18] R. Szeliski and J. Coughlan, "Spline-based image registration," *Int. J. Comput. Vis.*, vol. 22, pp. 199–218, 1997.

[19] P. Moulin, R. Krishnamurthy, and J. Woods, "Multiscale modeling and estimation of motion fields for video coding," *IEEE Trans. Image Processing*, vol. 6, pp. 1606–1620, Dec. 1997.

[20] M. Unser, A. Aldroubi, and M. Eden, "Recursive regularization filters: Design, properties, and applications," *IEEE Trans. Pattern Anal. Machine Intell.*, vol. 13, pp. 272–277, Mar. 1991.

[21] I. J. Schoenberg, *Cardinal Spline Interpolation*. Philadelphia, PA: SIAM, 1973.

[22] M. Unser, A. Aldroubi, and M. Eden, "B-spline signal processing: Part I—Theory," *IEEE Trans. Signal Processing*, vol. 41, pp. 821–832, Feb. 1993.

[23] ——, "B-spline signal processing: Part II—Efficient design and applications," *IEEE Trans. Signal Processing*, vol. 41, pp. 834–848, Feb. 1993.

[24] L. L. Schumaker, *Spline Functions Basic Theory*. New York: Wiley, 1981.

[25] Yu. Lyubarskii and W. R. Madych, "The recovery of irregularly sampled band limited functions via tempered splines," *J. Func. Anal.*, vol. 125, no. 1, pp. 201–222, Oct. 1994.

[26] A. Aldroubi, M. Unser, and M. Eden, "Cardinal spline filters: Stability and convergence to the ideal sinc interpolator," *Signal Process.*, vol. 28, no. 2, pp. 127–138, 1992.

[27] C. E. Shannon, "Communication in the presence of noise," *Proc. IRE*, vol. 37, pp. 10–21, Jan. 1949.

[28] G. Wahba, *Spline Models for Observational Data*. Philadelphia, PA: SIAM, 1990.

[29] K. Rohr, H. S. Stiehl, R. Sprengel, W. Beil, T. M. Buzug, J. Weese, and M. H. Kuhn, "Point-based elastic registration of medical image data using approximating thin-plate splines," in *Visualization in Biomedical Computing*, K. H. Höhne and R. Kikinis, Eds. New York: Springer-Verlag, 1996, pp. 297–306.

[30] J. Kybic, P. Thévenaz, A. Nirkko, and M. Unser, "Unwarping of unidirectionally distorted EPI images," *IEEE Trans. Med. Imag.*, vol. 19, pp. 80–93, Feb. 2000.

[31] A. W. Toga, Ed., *Brain Warping*. San Diego, CA: Academic, 1999.

[32] J. Maltz, R. De Mello Koch, and A. Willis, "Reproducing kernel Hilbert space method for optimal interpolation of potential field data," *IEEE Trans. Image Processing*, vol. 7, pp. 1725–1730, Dec. 1998.

[33] A. K. Jain, *Fundamentals of Digital Image Processing*. Englewood Cliffs, NJ: Prentice-Hall, 1989.

[34] F. Natterer, *The Mathematics of Computerized Tomography*. New York: Wiley, 1986.

[35] F. F. Rashid, K. J. R. Liu, C. A. Berenstein, and D. Walnut, "Wavelet-based multiresolution local tomography," *IEEE Trans. Med. Imag.*, pp. 1412–1430, Oct. 1997.

[36] W. R. Madych and S. A. Nelson, "Polynomial based algorithms for computed tomography," *SIAM J. Appl. Math.*, no. 1, pp. 157–185, Feb. 1983.

[37] J. Kybic, T. Blu, and M. Unser, "Variational approach to tomographic reconstruction," *Proc. SPIE*, Feb. 2001.

Jan Kybic (M'00) was born in Prague, Czech Republic, in 1974. He received the Mgr. (B.Sc.) and Ing. (M.Sc.) degrees with honors from the Czech Technical University, Prague, in 1996 and 1998, respectively. In 2001, he received the Ph.D. degree in biomedical image processing from Ecole Polytechnique Federale de Lausanne (EPFL), Lausanne, Switzerland, for his thesis on elastic image registration using parametric deformation models.

He is now with INRIA, Sophia-Antipolis, France. His research interests include signal and image processing in general, image registration, splines and wavelets, speech processing and enhancement, computer vision, numerical methods, algorithm theory, and control theory.

Thierry Blu (M'96) was born in Orléans, France, in 1964. He received the Diplôme d'ingénieur" from École Polytechnique, Paris, France, in 1986 and the M.Sc. degree from Télécom Paris (ENST), in 1988. He received the Ph.D. in electrical engineering from ENST in 1996 for a study on iterated rational filterbanks applied to wideband audio coding.

He is currently with the Biomedical Imaging Group, Swiss Federal Institute of Technology (EPFL), Lausanne, Switzerland, on leave from the France Télécom National Center for Telecommunications Studies (CNET), Issy-les-Moulineaux, France. His research interests include (multi)wavelets, multiresolution analysis, multirate filterbanks, approximation and sampling theory, psychoacoustics, etc.

Michael Unser (M'89–SM'94–F'99) received the M.S. (summa cum laude) and Ph.D. degrees in electrical engineering in 1981 and 1984, respectively, from the Swiss Federal Institute of Technology (EPFL), Lausanne, Switzerland.

From 1985 to 1997, he was with the Biomedical Engineering and Instrumentation Program, National Institutes of Health, Bethesda, MD. He is now Professor and Head of the Biomedical Imaging Group at EPFL. His main research area is biomedical image processing. He has a strong interest in sampling theories, multiresolution algorithms, wavelets, and the use of splines for image processing. He is the author of 90 published journal papers in these areas. He was on the editorial board of *Signal Processing*.

Dr. Unser is an Associate Editor for the IEEE TRANSACTIONS ON MEDICAL IMAGING. He has been on the editorial boards the IEEE TRANSACTIONS ON IMAGE PROCESSING from 1992 to 1995 and the IEEE SIGNAL PROCESSING LETTERS from 1994 to 1998. He serves as regular chair for the SPIE Conference on Wavelets, which has been held annually since 1993. He received the 1995 Best Paper Award and the 2000 Magazine Award from the IEEE Signal Processing Society.